Electron Microscopic and Immunohistochemical Examination of the Effect of 2-Aminoethoxydiphenyl Borate on Optic Nerve Injury in A Rat Model

Tuba Demirci[1], Nuray Bilge[2], Metin Ucar[3], Ozlem Ozgul Abuc[1], Hilal Atilay[1]

ABSTRACT

Objective: We conducted this study to explore the possible protective effect of 2-aminoethoxydiphenyl borate (2-APB) on experimentally induced optic nerve injury in an acute ischemia-reperfusion (AIR) model.

Materials and Methods: A total of 30 Wistar albino rats were randomly divided into sham, AIR, and AIR+treatment (AIR10) groups. In the sham group, AIR model was not created. In the AIR group, AIR model was created without the administration of drug. In the AIR10 group, 2-APB was administered 10 min before reperfusion.

Results: Tissue samples were subjected to histological, immunohistochemical, and electron microscopic procedures. Histopathological examination revealed intense hypertrophic cells, more glial cells, capillary dilatation, and intense demyelination areas in the AIR group compared to those in the sham and AIR10 groups. Immunohistochemical staining demonstrated an increase in Orai1 and STIM1 immunoreactivity in the AIR group but less intense staining in the AIR10 group. Electron microscopy revealed injury in optic nerve axons in the AIR group, whereas this type of injury occurred to a lesser extent in the AIR10 group.

Conclusion: In rats, store-operated Ca^{2+} entry in the cell had an essential role in optic nerve ischemia-reperfusion injury, and 2-ABP may have a protective effect on optic nerve injury caused due to AIR.

Keywords: Calcium channels, 2-aminoethoxydiphenyl borate, optic nerve injury

Cite this article as: *Demirci T, Bilge N, Ucar M, Ozgul Abuc O, Atilay H. Electron Microscopic and Immunohistochemical Examination of the Effect of 2-Aminoethoxydiphenyl Borate on Optic Nerve Injury in A Rat Model. Eurasian J Med 2020; 52(1): 61-6.*

[1]Department of Histology and Embryology, Atatürk University School of Medicine, Erzurum, Turkey
[2]Department of Neurology, Ataturk University School of Medicine, Erzurum, Turkey
[3]Department of Ophthalmology, Regional Training and Research Hospital, Erzurum, Turkey

Received: April 7, 2019
Accepted: October 17, 2019

Correspondence to: Tuba Demirci
E-mail: drtubademirci@hotmail.com

DOI 10.5152/eurasianjmed.2020.19089

Introduction

Ischemic injury to the retina and the optic nerve is frequently observed in ocular diseases. Severe ischemic damage leads to almost complete and irreversible vision loss [1]. After a ischemia-reperfusion injury, the damage caused to the optic nerve results in painless vision loss and subsequent deterioration in the normal nerve structure, retinal ganglion cell death, and permanent vision loss [2, 3]. One of the most commonly used models for investigating the molecular mechanism involved in optic nerve damage and the possible therapeutic strategies is the ischemia-reperfusion rat model, which is created by increased acute intraocular pressure. Recent studies have reported that excitatory amino acids with neurotoxic properties and molecular mediators, such as free oxidative radicals, play a role in retinal and optic nerve ischemia-reperfusion injury caused due to elevated acute intraocular pressure in rats [1, 4]. However, the mechanisms responsible for neuronal death after an ischemic-axonal injury in optic neuropathies induced in animal models have still not been fully elucidated. Therefore, the treatment of optic nerve damage continues to represent an important problem, and although complex and invasive novel treatment methods have been attempted in addition to classical treatment methods, the desired success has not been achieved.

Store-operated calcium (Ca^{2+}) channels are commonly found in the central nervous system and other tissues, such as the liver and heart, and have been reported to play a role in store-operated Ca^{2+} entry (SOCE) [5-8]. In a recent study, in which global ischemia was induced in rats, the role of store-operated channel proteins (STIM1 and Orai1) associated with Ca^{2+} loading in inducing delayed neuronal death was investigated in the neurons of the hippocampus. It was observed that suppression of SOCE with STIM1 siRNA in the early post-ischemic period resulted in a significant inhibition of the expression of STIM1 and Orai1, a decrease in intracellular Ca^{2+} concen-

tration in neurons, and an improvement in the neurological functions of rats. In other words, these findings imply that an overexpression of STIM1 and Orai1 is responsible for excessive Ca^{2+} entry into the cell as a result of ischemic injury and an inhibition of this entry increases neuronal survival. These data suggest that SOCE represents another mechanism besides excitotoxicity that is responsible for neuronal cell death in ischemic injury [5]. An another study also demonstrated that SOCE inhibition could reduce apoptosis in an ethanol-induced liver injury model [6].

2-Aminoethoxydiphenyl borate (2-APB), which inhibits Ca^{2+} release by blocking IP3 receptors in the endoplasmic reticulum (ER), has been extensively used to reduce Ca^{2+} release [9]. 2-APB exerts an effect of altering the IP3-induced Ca^{2+} release and can pass through the ER membrane. The difference between 2-APB and other antagonists that release Ca^{2+} through IP3 is that 2-APB inhibits Ca^{2+} channels present on the plasma membrane or intracellular vesicles. In this respect, 2-APB is the first IP3 modulator that does not affect Ca^{2+} entry from outside the cell [10, 11]. In our literature review, we observed that relatively few studies have explored the effect of the relationship between Ca^{2+} release from the ER and SOCE on optic nerve injury. We found no study in the literature that investigated the role of SOCE in optic nerve injury and the effect of 2-APB on this injury. Therefore, we conducted this study to analyze STIM1 and Orai1 via immunohistochemical examination to determine the role of SOCE in optic nerve injury after ocular ischemia-reperfusion and to evaluate the optic nerve structure by electron microscopy and histopathology. We also investigated the possible protective and therapeutic effects of the SOCE inhibitor 2-APB on optic nerve injury.

Materials and Methods

Animals

A total of 30 Wistar albino rats (aged 10-12 weeks) weighing approximately 250-300 g were used in this study. Animal care and experimental procedures were performed after obtaining the approval of the Local Ethics Council of Animal Experiments.

Experimental procedure

Rats were randomly divided into the following three groups: sham, acute ischemia-reperfusion (AIR), and AIR10, with 10 animals in each group. All rats were administered general anesthesia with ketamine (100 mg/kg; Ketalar; Pfizer) and chlorpromazine (25 mg/kg; Largactil; Eczacıbaşı), and topical anesthesia was achieved using 0.5% proparacaine (Alcaine; Alcon) drops in the right eyes. The eyes were then dilated using 1% cyclopentolate (Siklоplejin; Abdi İbrahim), and saline solution was injected into the anterior chamber using a 30-gage cannula. Intraocular pressure was not elevated in the sham group, in which the animals were injected with the needle, and the needle was removed. In the AIR group, a serum bottle was placed at a height of 200 cm from the rat for 60 min to increase the intraocular pressure to at least 120 mmHg and reperfusion was obtained. In the AIR10 group, 2-APB (Sigma-Aldrich) was intraperitoneally administered at a dose of 4 mg/kg 10 min before reperfusion [12]. After 3 days, the rats were sacrificed under anesthesia. Enucleation was performed on the right eyes of the rats, and the optic nerves were subjected to routine histological and electron microscopic procedures.

Histological procedure

The optic nerve tissues were fixed in 10% formalin solution for 48 h, after which the formalin was removed by washing in tap water. Tissues were then dehydrated by passing through an ethanol series with increasing concentrations and made transparent with xylene. Sections measuring 4-5 µm in thickness were prepared from the optic nerves embedded in paraffin using a microtome (Leica RM2235, Leica Instruments, Nussloch, Germany). Then, the sections were stained with hematoxylin–eosin (H–E) and toluidine blue (Sigma-Aldrich) and examined under a light microscope (Nikon, Eclipse-600, Tokyo, Japan).

The number of glial cells in the H–E-stained sections were counted and calculated by a Stereo-Investigator system (Microbrightfield, vs. 9.0, Colchester, VT, CA, USA) using the optical fractionator method [13]. This system consists of a light microscope with an attached camera, a motorized system that moves the microscope tray, and a computer software that controls the remaining apparatus. In this system, after placing the slide on the microscope tray, the image is reflected on the monitor, and the limits of the area to be measured are determined using the software. When the area to be measured is determined, cell counts are performed, while the step intervals on the x and y axes are progressed or advanced at a random angle with independent count frames separated from each other. The numerical density of glial cells in each μm^3 was calculated using the formula $Nd=TM/CFA \times NSS$ [Nd, numerical density; TM, counted total markers; CFA, counting frame area (XY) (μm^2); and NSS, the number of sampling sites][14].

Electron microscopy procedure

For electron microscopic examination of the optic nerve, 1 mm^3 tissue samples obtained from the rats were fixed with glutaraldehyde, followed by postfixation at 4°C in osmium tetroxide for 2 h. The sections were dehydrated by passing through a graded alcohol series, treated with propylene oxide, and then embedded in epoxy resin. Semi-thin sections measuring 1-2 µm in thickness prepared using an ultramicrotome (LKB NOVA, Bromma, Sweden) were stained with toluidine blue and then analyzed under a Nikon Eclipse-600 (Tokyo, Japan) light microscope equipped with a camera. Ultrathin sections measuring 70-80 nm in thickness placed on the grids (S162 grupPelco, CA, USA) were subjected to ultrastructural examination under a transmission electron microscope (100 SX Jeol, Tokyo, Japan), and digital images were obtained for all groups.

Immunohistochemical procedure

The sections were deparaffinized, passed through a graded ethanol series with decreasing concentrations, and then washed in distilled water. For retrieval, the antigen was boiled in ethylenediaminetetraacetic acid (EDTA) in a 90°C oven for 20 min. It was then placed in 3% hydrogen peroxide (H_2O_2) for 15 min, and endogenous peroxides were blocked. The sections were then incubated at room temperature with drops of Orai1 (Santa Cruz; dilution 1/100) and STIM1 (Santa Cruz; dilution 1/100) antibodies (no primary antibody was added to the negative control sections) for 60 min. Subsequently, secondary antibodies and 3,3′-diaminobenzidine were applied to the sections, and background staining was performed with hematoxylin, after which the sections were examined under a light microscope (Nikon, Eclipse-600, Tokyo, Japan). The intensity of immunoreactivity to STIM1 and Orai1 proteins in the optic nerve tissue was evaluated using a semi-quantitative method [15], wherein scoring was performed according to the ratio of positive cells as follows: 0=no positive cells, 1=<10% positive cells, 2=10%-50% positive cells, 3=51%-80% positive cells, and 4=>80% positive cells. The staining intensity was scored as follows: 0=no staining, 1=weak staining, 2=moderate staining, and 3=severe staining. Thereafter, an immunoreactivity score of 0-12 was obtained by multiplying the staining intensity score (0-3) with the ratio of positive cells (0-4).

Statistical Analysis

The Statistical Package for the Social Sciences (SPSS) version 20.0. software (IBM Corp.; Armonk, NY, USA) was used for the statistical analysis of the data. Multiple comparisons were

conducted using the Kruskal–Wallis test. The Mann–Whitney U test was used for binary comparisons. A $p<0.001$ was considered as statistically significant.

Results

Histopathological examination

The H–E-stained tissue sections in the sham group demonstrated normal myelinated nerve fibers, implying that the axon alignment was regular and the myelin sheath around the axon was normal. The nerve axons were tightly packed together and partially formed bundles, and between the bundles was the connective tissue with capillary vessels. Oligodendrocytes and astrocytes were found to be scattered within the nerve tissue (Figure 1a). Compared with the sham group, the number of glial cells in the AIR group increased significantly ($p<0.001$) (Table 1). Furthermore, there were distortion in the axon alignment and significant axonal degeneration. Swelling and vacuolar degeneration were prominent in the myelin sheaths of the axons. There was an increase in the connective tissue between the axons, along with dilatation of the vessels (Figure 1b). Intensive demyelination areas, axonal degeneration, and vacuolization were more prominent in sections stained with toluidine blue (Figure 1b1). The glial cell count was lower in the group treated with 2-ABP 10 min before reperfusion than that in the AIR group ($p<0.001$), but it was higher than that in the sham group ($p<0.001$). Injury findings such as demyelination areas, capillary dilatation, swelling of myelin sheaths, and vacuolar degeneration were less frequent in the AIR10 group (Figure 1c, 1c1).

Electron microscopy findings

In the sham group, optic nerve axons were aligned closely together and demonstrated a compact myelin structure (Figure 2a). In the injury groups, optic nerve axons were swollen and infrequently aligned, with abnormal proliferation of the neural connective tissue between the axons. In addition to axonal swelling, normal axonal appearance was impaired due to rapid division of axonal myelin sheaths. Particularly in the AIR group, myelin was disintegrated into lamellae. Compared to a normal optic nerve, the number of large axons decreased in the injury group, whereas that of small axons exhibited a relative increase (Figure 2b). Although normal myelinated axons were more frequent in the AIR10 group treated with 2-APB than in the AIR group, vacuoles of different shapes and sizes were observed in the axons. Furthermore, the neural connective tissue showed abnormal proliferation in both AIR and AIR10 groups, with higher proliferation being observed in the AIR group (Figure 2c).

Immunohistochemistry

Immunohistochemical examination was performed using the optic nerve tissues of rats from all three groups to evaluate the immunoreactivity to STIM1 and Orai1 in glial cells, which have a significant role in Ca^{2+} entry into cells. The immunoreactivity scores of STIM1 and Orai1 were increased significantly in the ischemia-reperfusion groups compared to those in the sham group ($p<0.001$). After treatment with 2-APB following the ischemia-reperfusion injury, there was a significant decrease in both STIM1 and Orai1 immunoreactivity scores ($p<0.001$); how-

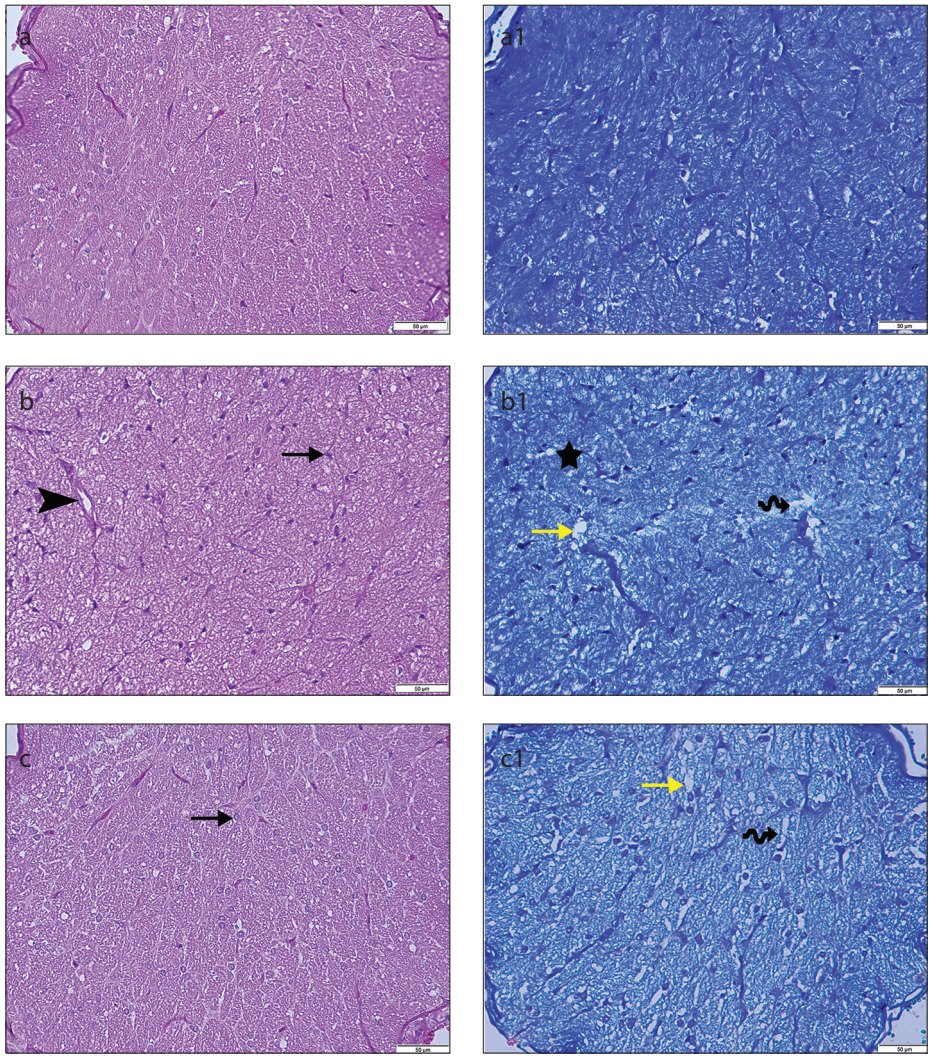

Figure 1. a-c Light photomicrographs of optic nerve tissues stained with Hematoxylin-eosin (a-c) and toluidine blue (a1-c1). Black arrow: glial cell, yellow arrow: vacuolar degeneration, arrow head: dilation of the capillaries, ⋆: glial cell increase and ∼: demyelination areas. (a-a1) Sham groups; (b-b1) AIR groups; (c-c1) AIR10 group. Bars: 50 µm.

Table 1. Numerical densities and immunoreactivity scores of glial cells in the control and experimental groups

Groups	Glial cells (n/µ3) (Mean±SD)	Orai1 IRS (Mean±SD)	STIM1 IRS (Mean±SD)
Sham	$3.54\times10^{-4}\pm0.18\times10^{-4}$	1.2±0.42	1.3±0.48
AIR	$4.52\times10^{-4}\pm0.16\times10^{4}$ [a,b]	7.8±1.32[a,b]	8.5±2.22[a,b]
AIR10	$3.97\times10^{-4}\pm0.15\times10^{-4}$ [a,c]	3.0±1.41[a,c]	3.7±1.42[a,c]

SD: standard deviation; IRS: immunoreactivity score; AIR: acute ischemia-reperfusion; AIR10: acute ischemia-reperfusio+4 mg/kg 2-APB
[a]Significantly increased when compared with the sham group ($p<0.01$)
[b]Significantly decreased when compared with the AIR10 group ($p<0.01$)
[c]Significantly increased when compared with the AIR group ($p<0.01$)

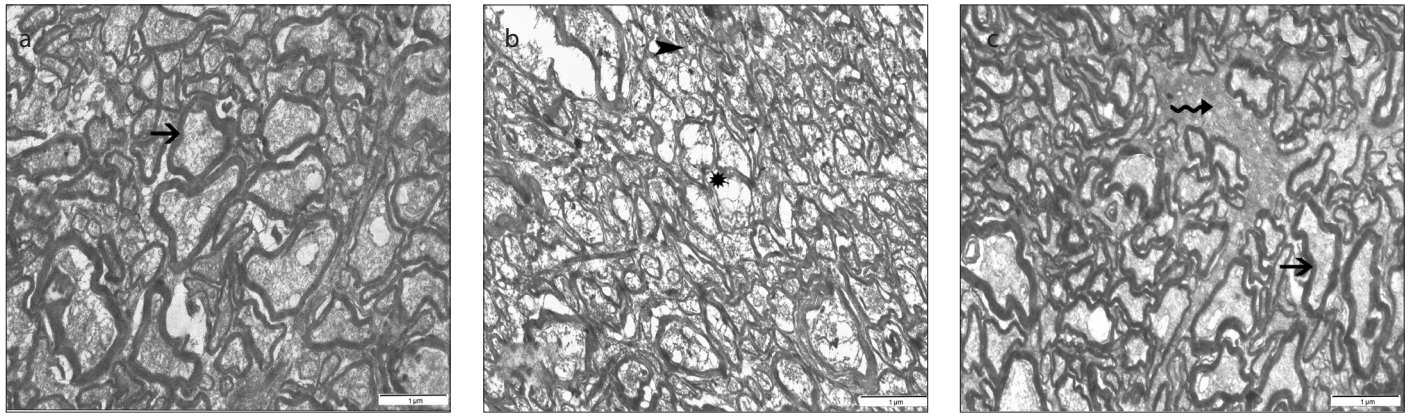

Figure 2. a-c. Electron photomicrographs of optic nerve tissues. (a) Myelinated axons in the sham group. (b) Separation of the myelin sheath (arrowhead), deterioration of axonal shape and demyelination areas (asterisks) in the AIR group. (c) Abnormal proliferation of connective tissue (curved arrow) between the normal myelinated axons (arrow) in the AIR10 group. Bars: 1 µm.

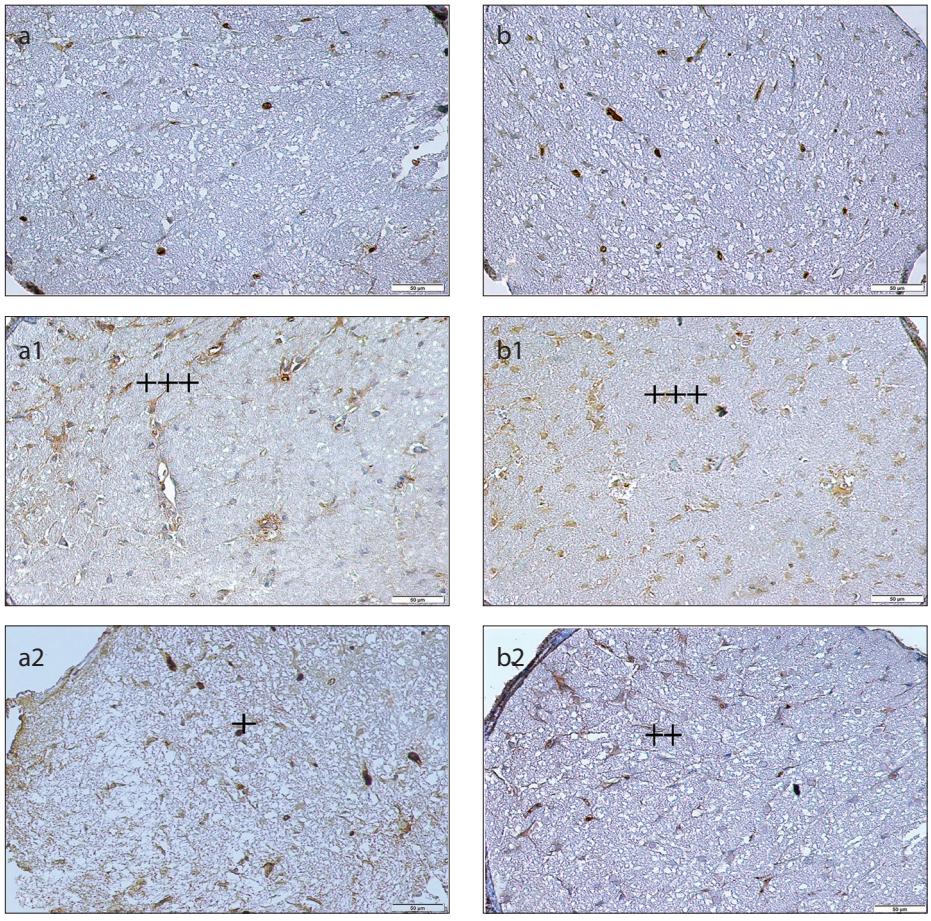

Figure 3. a, b Light photomicrographs of Orai1 (a-a2) and STIM1 (b-b2) immunohistochemistry of optic nerve tissues. (a, b) Sham groups; (a1-b1) AIR groups; (a2-b2) AIR10 groups. (+), mild staining; (++), moderate staining; (+++), severe staining. Bars: 50 µm.

ever, these scores were still higher than those in the sham group ($p<0.001$) (Table 1, Figure 3).

Discussion

Progressive and irreversible vision loss caused due to optic nerve damage is an important health concern. Diseases such as vascular occlusion, hypertension, diabetic retinopathy, glaucoma, and acute ocular hypertension lead to ischemic injury of the optic nerve. Severe ischemic events have been reported to cause almost complete and irreversible loss of visual function [1]. Furthermore, experimental animal models have shown that retinal ischemia was induced by increased intraocular pressure [16, 17]. An increased intraocular pressure can result in optic nerve injury and axonal loss [18]. Several studies have also reported the presence of demyelination areas in the optic nerve in retinal ischemia and glaucoma models caused due to an increased intraocular pressure [19, 20]. In the present study also, it was observed that an increased intraocular pressure caused damage to the optic nerve, as indicated by the presence of swelling and vacuolar degeneration in the myelin sheaths of the axons, the increased connective tissue between the axons, and the dilatation of the vessels. Our histopathological findings of the optic nerve injury caused due to increased intraocular pressure were in accordance with the literature. The deterioration of these findings in the 2-APB-treated group suggested that the damage is related to SOCE-mediated calcium entry into the cell.

Recent studies have demonstrated that SOCE is essential for both the regeneration of intracellular ER Ca^{2+} stores and the maintenance of ATP-mediated Ca^{2+} signal in optic nerve glial cells [21, 22]. It has been reported that the ATP-mediated astroglial signal affects the homeostatic and metabolic support functions of glial cells [23]. In a study conducted by Joos et al. [24], glial cell activation, including astrocytes, was observed during optic nerve degeneration. In our study, we also observed an increased number of glial cells in the AIR injury group. This finding and the presence of intensive connective tissue in the areas between axons indicated glial cell activation during injury. However, in the group treated with 2-APB, the number of glial cells was less. This could be because 2-APB, an SOCE inhibitor, suppressed the proliferation of glial cells by inhibiting SOCE-mediated Ca^{2+} entry into the cell following ischemia.

Pelit et al. [25] created an ischemic optic neuropathy model by inducing retrobulbar hematoma in rabbits and performed an electron microscopic examination of the optic nerves, which revealed deterioration of the concentric lamellar structure of myelin sheaths and irregular deteriorations due to the separation of myelin lamellae. In another study, May [26] investigated optic nerve

injury in patients with primary open-angle glaucoma by ultrastructural methods and observed the presence of numerous small and abnormal sized axons and degenerated areas of myelin in the majority of areas. Nitza Goldenberg-Cohen et al. [3] also induced preischemic optic neuropathy in mice in a similar manner and conducted an electron microscopic investigation, which demonstrated axonal degeneration and swelling. In our study, the electron microscopic examination demonstrated the presence of axonal damage, particularly in the AIR group, which is similar to that mentioned in the literature. In the optic nerve sections of the injury groups, myelins were disintegrated into lamellae, and nonmyelinated and thin myelinated axons were present. The optic nerve axons were swollen and intermittently aligned, and the neural connective tissue between the axons showed abnormal proliferation. The administration of 2-APB 10 min before reperfusion significantly reduced this injury, and this amelioration was detected at the ultrastructural level in the present study. Axonal degeneration was detected less frequently in the treatment group, and axons with an intact myelin sheath were observed prominently.

Cells maintain their intracellular Ca^{2+} at certain levels through various mechanisms. In several cell types, SOCE regulates the increase in cytosolic Ca^{2+} concentration, which is critical for the regulation of various cellular functions, such as secretion, apoptosis, and proliferation. Under physiological conditions, STIM1 receptors on the ER are stimulated in response to G protein-linked receptors on the plasma membrane, which are activated due to various reasons. The stimulation of STIM1 receptors also stimulates Ca^{2+} release, resulting in SOCE or Ca^{2+} entry into cells and allowing Ca^{2+} concentration to increase rapidly in the cytoplasm [27, 28]. A recent study involving the induction of global ischemia in rats investigated the role of STIM1 and Orai1 proteins associated with Ca^{2+} loading in inducing delayed neural death by examining the neurons of the hippocampus after ischemia. It was observed that in the early postischemic period, the suppression of SOCE by STIM1 siRNA resulted in a significant inhibition of the expression of STIM1 and Orai1 and a decreased intracellular Ca^{2+} concentration in neurons; there was also an improvement in the neurological functions of rats after the injection of STIM1 siRNA. These findings imply that the overexpression of STIM1 and Orai1 is responsible for excessive Ca^{2+} entry into the cell as a result of ischemic injury, and inhibiting this entry increases neuronal survival. These data further suggest that SOCE is based on another mechanism besides excitotoxicity that is responsible for causing neuronal cell death in ischemic injury [5]. In our study, we found a significant increase in the immunoreactivity scores of both STIM1 and Orai1 in glial cells during AIR injury compared to that in the control group. These data indicate that increased expression of STIM1 and Orai1 may be related to increased glial cell activation. In the glial cells, ischemia-reperfusion injury led to an increase in the expression of STIM1 and Orai1, and as a result of this elevation, there was an increase in the SOCE-mediated Ca^{2+} entry into the cell. Reducing this increase via 2-APB treatment, an SOCE inhibitor, confirmed that SOCE-mediated Ca^{2+} entry into the glial cells increased during optic nerve injury.

This study has some potential limitations. The SOCE-mediated Ca^{2+} entry into the cell was determined by measuring the expression of SOCE-related receptors using immunohistochemical techniques. Determining the intracellular calcium level using the patch clamp method would provide quantitative results. However, as the patch clamp is an expensive system and not available in our laboratory, only the SOCE-related receptors were evaluated immunohistochemically. It was also possible to examine the myelin sheath and other neural elements around the nerve fibers using our immunohistochemical technique. However, in our study, we focused on the electron microscopic examination, which is an expensive method and examines the tissue in an ultrastructural manner. We hope that our study findings will guide those researchers investigating this area.

In conclusion, our results demonstrate that SOCE plays a role in optic nerve damage in AIR. Moreover, 2-APB inhibits the increased expression of STIM1 and Orai1 in the optic nerve during AIR and may have a protective effect.

Ethics Committee Approval: Ethics committee approval was received for this study from the Local Ethics Council of Animal Experiments of Ataturk University.

Informed Consent: N/A.

Peer-review: Externally peer-reviewed.

Author Contributions: Concept – T.D., N.B., M.U.; Design - T.D., N.B., M.U.; Supervision - T.D.; Resources - T.D.; Materials – T.D., H.A.; Data Collection and/or Processing - T.D., N.B., M.U., H.A., O.O.A.; Analysis and/or Interpretation - T.D., O.O.A.; Literature Search - T.D.; Writing Manuscript - T.D., N.B., M.U., O.O.A., H.A.; Critical Review - T.D., N.B.

Conflict of Interest: The authors have no conflicts of interest to declare.

Financial Disclosure: The authors declared that this study has received no financial support.

References

1. Grozdanic SD, Sakaguchi DS, Kwon YH, Kardon RH, Sonea IM. Functional characterization of retina and optic nerve after acute ocular ischemia in rats. Invest Ophthalmol Vis Sci 2003; 44: 2597-605. [CrossRef]
2. Yoshida K, Behrens A, Le-Niculescu H, et al. Amino-terminal phosphorylation of c-Jun regulates apoptosis in the retinal ganglion cells by optic nerve transection. Invest Ophthalmol Vis Sci 2002; 43: 1631-5.
3. Goldenberg-Cohen N, Guo Y, Margolis F, Cohen Y, Miller NR, Bernstein SL. Oligodendrocyte dysfunction after induction of experimental anterior optic nerve ischemia. Invest Ophthalmol Vis Sci 2005; 46: 2716-25. [CrossRef]
4. Shibuki H, Katai N, Yodoi J, Uchida K, Yoshimura N. Lipid peroxidation and peroxynitrite in retinal ischemia-reperfusion injury. Invest Ophthalmol Vis Sci 2000; 41: 3607-14.
5. Zhang M, Song JN, Wu Y, et al. Suppression of STIM1 in the early stage after global ischemia attenuates the injury of delayed neuronal death by inhibiting store-operated calcium entry-induced apoptosis in rats. Neuroreport 2014; 25: 507-13. [CrossRef]
6. Cui R, Yan L, Luo Z, Guo X, Yan M. Blockade of store-operated calcium entry alleviates ethanol-induced hepatotoxicity via inhibiting apoptosis. Toxicol Appl Pharmacol 2015; 287: 52-66. [CrossRef]
7. Collins HE, Zhu-Mauldin X, Marchase RB, Chatham JC. STIM1/Orai1-mediated SOCE: current perspectives and potential roles in cardiac function and pathology. Am J Physiol Heart Circ Physiol 2013; 305: H446-H58. [CrossRef]
8. Avila-Medina J, Mayoral-Gonzalez I, Dominguez-Rodriguez A, et al. The Complex Role of Store Operated Calcium Entry Pathways and Related Proteins in the Function of Cardiac, Skeletal and Vascular Smooth Muscle Cells. Front Physiol 2018; 9: 257. [CrossRef]
9. Peppiatt CM, Collins TJ, Mackenzie L, et al. 2-Aminoethoxydiphenyl borate (2-APB) antagonises inositol 1, 4, 5-trisphosphate-induced calcium release, inhibits calcium pumps and has a use-dependent and slowly reversible action on store-operated calcium entry channels. Cell Calcium 2003; 34: 97-108. [CrossRef]
10. Bilmen JG, Michelangeli F. Inhibition of the type 1 inositol 1, 4, 5-trisphosphate receptor by 2-aminoethoxydiphenylborate. Cell Signal 2002; 14: 955-60. [CrossRef]
11. Iwasaki H, Mori Y, Hara Y, Uchida K, Zhou H, Mikoshiba K. 2-Aminoethoxydiphenyl borate (2-APB) inhibits capacitative calcium entry independently of the function of inositol 1, 4, 5-trisphosphate receptors. Recept Channels 2001; 7: 429-39.
12. Sari E, Aksit H, Erken HA, et al. Protective effect of 2-APB on testicular ischemia-reperfusion injury in rats. J Urol 2015; 193: 1036-41. [CrossRef]
13. Gundersen H, Bagger P, Bendtsen T, et al. The new stereological tools: disector, fractionator, nucleator and point sampled intercepts and their

use in pathological research and diagnosis. APMIS 1988; 96: 857-81. [CrossRef]
14. Arabaci T, Kose O, Kizildag A, Albayrak M, Cicek Y, Kara A. Role of nuclear factor kappa-B in phenytoin-induced gingival overgrowth. Oral Dis 2014; 20: 294-300. [CrossRef]
15. Fedchenko N, Reifenrath J. Different approaches for interpretation and reporting of immunohistochemistry analysis results in the bone tissue-a review. Diagn Pathol 2014; 9: 221. [CrossRef]
16. Lagreze WA, Knörle R, Bach M, Feuerstein TJ. Memantine is neuroprotective in a rat model of pressure-induced retinal ischemia. Invest Ophthalmol Vis Sci 1998; 39: 1063-6.
17. Osborne NN. Memantine reduces alterations to the mammalian retina, in situ, induced by ischemia. Vis Neurosci 1999; 16: 45-52. [CrossRef]
18. Sun SW, Liang HF, Le TQ, Armstrong RC, Cross AH, Song SK. Differential sensitivity of in vivo and ex vivo diffusion tensor imaging to evolving optic nerve injury in mice with retinal ischemia. Neuroimage 2006; 32: 1195-204. [CrossRef]
19. Orgül S, Cioffi GA, Wilson DJ, Bacon DR, Van Buskirk EM. An endothelin-1 induced model of optic nerve ischemia in the rabbit. Invest Ophthalmol Vis Sci 1996; 37: 1860-9.
20. Song SK, Sun SW, Ju WK, Lin SJ, Cross AH, Neufeld AH. Diffusion tensor imaging detects and differentiates axon and myelin degeneration in mouse optic nerve after retinal ischemia. Neuroimage 2003; 20: 1714-22. [CrossRef]
21. James G, Butt A. P2X and P2Y purinoreceptors mediate ATP-evoked calcium signalling in optic nerve glia in situ. Cell Calcium 2001; 30: 251-9. [CrossRef]
22. Papanikolaou M, Lewis A, Butt A. Store-operated calcium entry is essential for glial calcium signalling in CNS white matter. Brain Struct Funct 2017; 222: 2993-3005. [CrossRef]
23. Butt AM, Fern RF, Matute C. Neurotransmitter signaling in white matter. Glia 2014; 62: 1762-79. [CrossRef]
24. Joos KM, Li C, Sappington RM. Morphometric changes in the rat optic nerve following short-term intermittent elevations in intraocular pressure. Invest Ophthalmol Vis Sci 2010; 51: 6431-40. [CrossRef]
25. Pelit A, Haciyakupoglu G, Zorludemir S, Mete U, Daglioglu K, Kaya M. Preventative effect of deferoxamine on degenerative changes in the optic nerve in experimental retrobulbar haematoma. Clin Exp Ophthalmol 2003; 31: 66-72. [CrossRef]
26. May CA. Specific Densified Regions in the Postlaminar Human Glaucomatous Optic Nerve. Open Ophthalmol J 2015; 9: 20-4. [CrossRef]
27. Parekh AB, Putney Jr JW. Store-operated calcium channels. Physiol Rev 2005; 85: 757-810. [CrossRef]
28. Vazquez G, Wedel BJ, Bird GSJ, Joseph SK, Putney JW. An inositol 1, 4, 5-trisphosphate receptor-dependent cation entry pathway in DT40 B lymphocytes. EMBO J 2002; 21: 4531-8. [CrossRef]